Supporting Information

Wei et al. 10.1073/pnas.1013499108

SI Methods

Increasing the Size of the Matrix. In Fig. 1*B*, at 4 d the ratio of motile to nonmotile increased with the diffusion coefficient of the motile strain, D_{M}, and then declined as D_{M} increased. We suggested that this decline is "an artifact of the Neumann (zero flux) boundary condition used in the simulation" and this effect would not be obtained if the simulated Petri dish was larger. Support for this suggestion can be seen in Fig. S1, where the size of the matrix is fourfold greater than that in Fig. 1.

Random Distribution of Cells. In Fig. 3 we presented experimental evidence that even when the populations are initiated with a random distribution of motile (M) and nonmotile (N) cells, in the physically structured (agar) habitat the motile cells would have an advantage over the nonmotile ones. Whereas this is also the case for the PDE model, the advantage of the motile strain in the simulations is not as great as that observed in our experiments. This can be seen in Fig. S2*A*. When the M and N cells are randomly dispersed throughout the matrix, the motile cells have only a modest advantage. The reason for this is that it there is little competition between the N and M cells for some time. The motile cells have a greater advantage over the nonmotile cells, when 50 cells of each type are distributed as pairs (Fig. S2*B*).

Numerical Scheme to Solve the System of Partial Differential Equations and its Stability and Convergence. In this section we present our numerical scheme to numerically solve the system of nonlinear partial differential equations and prove that the scheme is stable and converges to the actual solution. We use an implicit scheme, similar in spirit to the backward Euler scheme used to solve ordinary differential equations (ODEs). The well-known explicit Euler scheme to solve the ODE $y' = f(t, y)$ with time step τ is $y_{n+1} = y_n + \tau f(t_n, y_n)$. The right-hand side is simply evaluated at time step n and determines the numerical approximation y_{n+1} at time step $n + 1$. Although easy to implement, such methods have a critical time step size, frequently quite small, above which numerical instabilities and unreliable results manifest. The implicit or backward Euler scheme is $y_{n+1} = y_n + \tau f(t_{n+1}, y_{n+1})$. Note that y_{n+1} appears on both sides of the equation and thus requires using a numerical method to estimate. Although more complicated and costly to implement, implicit schemes in general tend to produce reliable results for large step sizes τ.

Numerical scheme. We discretize the system of partial differential equations

$$\frac{\partial b_{\mathrm{M}}}{\partial t} = D_{\mathrm{M}}\left(\frac{\partial^2 b_{\mathrm{M}}}{\partial x^2} + \frac{\partial^2 b_{\mathrm{M}}}{\partial y^2}\right) + \frac{\alpha r}{r+k} b_{\mathrm{M}} \qquad \textbf{[S1]}$$

$$\frac{\partial b_{\mathrm{N}}}{\partial t} = D_{\mathrm{N}}\left(\frac{\partial^2 b_{\mathrm{N}}}{\partial x^2} + \frac{\partial^2 b_{\mathrm{N}}}{\partial y^2}\right) + \frac{\alpha r}{r+k} b_{\mathrm{N}} \qquad \textbf{[S2]}$$

$$\frac{\partial r}{\partial t} = D_r\left(\frac{\partial^2 r}{\partial x^2} + \frac{\partial^2 r}{\partial y^2}\right) - \frac{\nu r}{r+k}\left(b_{\mathrm{M}} + b_{\mathrm{N}}\right) \qquad \textbf{[S3]}$$

in time and space. The time steps are of the form $t_n = n\tau$ where $\tau > 0$ and the grid points on the "Petri dish" are of the form (ih, jh), where $h > 0$ and $i, j = 0, \ldots, S$.

We use a backward Euler scheme to discretize the time derivative in each of the three PDEs as follows:

$$\frac{\partial u}{\partial t} \approx \frac{u^{n+1} - u^n}{\tau}.$$

We also use a second-order central difference scheme to discretize the Laplacian operator (sum of second partial derivatives) in each of the three PDEs as follows:

$$\Delta u_{i,j} \approx \frac{1}{h^2}\delta^2 u_{i,j} = \frac{1}{h^2}\left(u_{i+1,j} + u_{i-1,j} + u_{i,j+1} + u_{i,j-1} - 4u_{i,j}\right).$$

Here δ denotes an operator and not a number.

Let $\lambda_{\mathrm{M}} = D_{\mathrm{M}}\tau/h^2$, $\lambda_{\mathrm{N}} = D_{\mathrm{N}}\tau/h^2$, where M and N denote motile and nonmotile strains, not indexes. We discretize Eqs. **S1** and **S2** by

$$-\lambda_{\mathrm{M}}\delta^2 b^{n+1}_{\mathrm{M},i,j} + \left(1 - \tau\frac{\alpha r^n_{i,j}}{k + r^n_{i,j}}\right) b^{n+1}_{\mathrm{M},i,j} = b^n_{\mathrm{M},i,j}$$

$$-\lambda_{\mathrm{N}}\delta^2 b^{n+1}_{\mathrm{N},i,j} + \left(1 - \tau\frac{\alpha r^n_{i,j}}{k + r^n_{i,j}}\right) b^{n+1}_{\mathrm{N},i,j} = b^n_{\mathrm{N},i,j}.$$

Note that at time $(n + 1)\tau$, the quantities $b^n_{\mathrm{M},i,j}$, $b^n_{\mathrm{N},i,j}$, and $r^n_{i,j}$ have already been computed.

To discretize Eq. **S3**, we replace the nonlinear Monod growth term

$$f(r) = \frac{\nu r}{k + r} \qquad \textbf{[S4]}$$

at time $(n + 1)\tau$ by its linearization and obtain

$$\begin{aligned} &-\lambda_r\delta^2 r^{n+1}_{i,j} + \left(1 + \tau\left(b^n_{\mathrm{M},i,j} + b^n_{\mathrm{N},i,j}\right) f'\left(r^n_{i,j}\right)\right) r^{n+1}_{i,j} \\ &\quad = \left(1 + \tau\left(b^n_{\mathrm{M},i,j} + b^n_{\mathrm{N},i,j}\right) f'\left(r^n_{i,j}\right)\right) r^n_{i,j} - \tau\left(b^n_{\mathrm{M},i,j} + b^n_{\mathrm{N},i,j}\right) f\left(r^n_{i,j}\right), \end{aligned} \qquad \textbf{[S5]}$$

where $\lambda_r = D_r\tau/h^2$ and $i, j = 1, \ldots, S - 1$. Note that the discretized equations at time $(n + 1)\tau$ are linear in b_{M}, b_{N}, and r.

We now incorporate the Neumann boundary conditions, corresponding to zero flux of bacteria or nutrient in out of the Petri dish, for b_{M}, b_{N}, and r in discretized form. For b_{M}, this yields the following system of linear equations:

$$\begin{cases} b^{n+1}_{\mathrm{M},0,j} - b^{n+1}_{\mathrm{M},1,j} = 0 \\ b^{n+1}_{\mathrm{M},S-1,j} - b^{n+1}_{\mathrm{M},S,j} = 0 \\ b^{n+1}_{\mathrm{M},i,0} - b^{n+1}_{\mathrm{M},i,1} = 0 \\ b^{n+1}_{\mathrm{M},i,S-1} - b^{n+1}_{\mathrm{M},i,S} = 0. \end{cases} \qquad \textbf{[S6]}$$

The equations for b_{N} and r are similar.

Combining all of the discretizations yields a *linear* system of equations that can be succinctly written as

$$\begin{aligned} A^n_{\mathrm{M}} b^{n+1}_{\mathrm{M}} &= l^n_{\mathrm{M}} \\ A^n_{\mathrm{N}} b^{n+1}_{\mathrm{N}} &= l^n_{\mathrm{N}} \\ A^n_r r^{n+1} &= l^n_r. \end{aligned} \qquad \textbf{[S7]}$$

The three matrices A^n_* on the left-hand side and the three vectors l^n_* on the right-hand side are all given at time $n\tau$, whereas the three vectors b^n_* on the left-hand sides are considered unknowns.

We use well-known numerical linear algebra techniques (1) that enable us to assume that the matrices are symmetric and positive. The matrices are also sparse, having only nonzero elements on the three block diagonals. We use the very fast conjugate gradient (CG) method to solve the linear systems, exploiting the sparsity. The implementation of the CG method with MatLab is so fast that preconditioning is unnecessary at these resolutions.

Stability and convergence. To guarantee a reliable numerical result using an explicit scheme requires choosing the time step τ to be of the order of h^2. If h is small, this has huge computational cost and there are potentially serious problems with round-off errors. Our implicit scheme avoids this problem and provides a reliable result with large τ.

We first prove that our algorithm for computing b_{M} and b_{N} is *stable* (1), in the sense that the errors made at one time step of the calculation do not cause the errors to increase as the computations are continued. Von Neumann introduced a procedure to verify the stability of finite difference schemes for linear systems of PDEs. Even though Eqs. **S1** and **S2** are not linear, at each time step our algorithm fixes the nonlinear Monod term and thus the equations are linear in b_{M} and b_{N}. This result enables us deduce stability via the Von Neumann method (1).

Theorem 0.0.1. *Our numerical scheme for solving Eqs.* **S1** *and* **S2** *is unconditionally stable*; *i.e., the choice of* τ *is independent of* h.

Proof. We closely follow the procedure in ref. 1. Our discretization of Eq. **S1** is

$$-\lambda_{\mathrm{M}}\delta^2 b_{\mathrm{M},i,j}^{n+1}+\left(1-\tau\frac{\alpha r_{i,j}^{n}}{k+r_{i,j}^{n}}\right)b_{\mathrm{M},i,j}^{n+1}=b_{\mathrm{M},i,j}^{n}.$$

Taking the spatial discrete Fourier transform of both sides yields the following expression for the Von Neumann amplification factor ρ,

$$\rho(\varepsilon,\eta)=1/\left(1+4\lambda_{\mathrm{M}}\left(\sin^2\frac{\varepsilon}{2}+\sin^2\frac{\eta}{2}\right)-\tau f(r^n)\right),$$

where $\widehat{b}_{\mathrm{M}}^{n+1}(\varepsilon,\eta)=\rho(\varepsilon,\eta)\widehat{b}_{\mathrm{M}}^{n}(\varepsilon,\eta)$, and thus the amplitude of each frequency in the solution, given by $\widehat{b}_{\mathrm{M}}^{n}(\varepsilon,\eta)$, is amplified by $\rho(\varepsilon,\eta)$ in one time step. Because $\alpha < 1$, the Monod term

$$f(r)=\frac{\alpha r}{k+r}\leq 1,$$

and thus

$$|\rho|\leq 1/(1-\tau)=1-\tau+O(\tau^2).$$

It follows from Von Neumann stability analysis that this scheme is unconditionally stable. A similar argument proves that the numerical scheme for Eq. **S2** is also unconditionally stable.

We cannot use the above technique to treat Eq. **S3** as a linear PDE in r and must deal directly with the nonlinearity. For this PDE we prove that the sup or ℓ_∞ norm of the numerical solutions are decreasing in time. We need the following lemma.

Lemma 0.0.2. *Consider the ordinary differential equation*

$$\frac{du}{dt}=-f(u),\;\; f(u)=\frac{u}{k+u},$$

where k *is a positive constant. Discretize this ODE as*

$$u^{n+1}=u^n-\tau\left[f(u^n)+f'(u^n)\left(u^{n+1}-u^n\right)\right]. \qquad \textbf{[S8]}$$

If $u^n\geq 0$ *for any time* $n\tau$, *then* $u^{n+1}\leq u^n$.

Proof. We write

$$\frac{u^{n+1}-u^n-\tau f(u^n)+\tau f'(u^n)u^n}{1+\tau f'(u^n)}=u^n-\frac{\tau f(u^n)}{1+\tau f'(u^n)}.$$

Because $\tau > 0$, $f(u^n)\geq 0$, and $f'(u^n) > 0$, it easily follows that $u^{n+1}\leq u^n$.

We now prove the monotonicity statement.

Theorem 0.0.3. *For the discretization of Eq.* **S3**, *if* $r_{i,j}^n\geq 0$ *for any* i, j, n, *then*

$$\max_{i,j} r_{i,j}^{n+1}\leq\max_{i,j} r_{i,j}^{n}.$$

Thus, the sup norm of the numerical solutions are decreasing in time.

Proof. Assume that for $(i,j)=(s,t), r_{s,t}^{n+1}=\max_{i,j} r_{i,j}^{n+1}$. Then

$$\lambda_r\delta^2 r_{s,t}^{n+1}+r_{s,t}^{n+1}=r_{s,t}^{n}-\tau\left(f\left(r_{s,t}^{n}\right)+f'\left(r_{s,t}^{n}\right)\left(r_{s,t}^{n+1}-r_{s,t}^{n}\right)\right)$$
$$\times\left(b_{\mathrm{M},s,t}^{n}+b_{\mathrm{N},s,t}^{n}\right).$$

Recalling that

$$\delta^2 r_{s,t}^{n+1}=r_{s+1,t}^{n+1}+r_{s-1,t}^{n+1}+r_{s,t-1}^{n+1}+r_{s,t+1}^{n+1}-4r_{s,t}^{n+1},$$

and because $r_{s,t}^{n+1}=\max_{i,j} r_{i,j}^{n+1}$ and $\lambda_r > 0$, it follows that

$$-\lambda_r\delta^2 r_{s,t}^{n+1}\geq 0.$$

This result implies that

$$r_{s,t}^{n+1}\leq r_{s,t}^{n}-\tau\left(f\left(r_{s,t}^{n}\right)+f'\left(r_{s,t}^{n}\right)\left(r_{s,t}^{n+1}-r_{s,t}^{n}\right)\right)\left(b_{\mathrm{N},s,t}^{n}+b_{\mathrm{M},s,t}^{n}\right).$$

It follows from Lemma 0.2 that

$$r_{s,t}^{n+1}\leq r_{s,t}^{n}.$$

Because $r_{s,t}^{n}\leq\max_{i,j} r_{i,j}^{n}$, we conclude that

$$\max_{i,j} r_{i,j}^{n+1}\leq\max_{i,j} r_{i,j}^{n}.$$

Note that the hypothesis requires $r_{i,j}^n\geq 0$ for all i, j, n. Our algorithm defines r to be 0 if it is below a very small threshold so this requirement is satisfied. Therefore, we conclude that the resource r at time $(n+1)\tau$ is bounded by the value of r at time $n\tau$.

Consistency is another key desired factor of a numerical algorithm; it guarantees that the smooth solution of the PDE is an approximate solution of the finite difference scheme. We now give the mathematical definition of consistency (1). We write a system of PDEs in compact form $Pu = f$, where P is a matrix containing partial derivatives.

Definition 1. Given a PDE $Pu = f$ and a finite difference scheme, $P_{k,h}{}^{v} = f_{k,h}$, the finite difference scheme is consistent with the PDE if for any smooth function $\phi(t,x)$

$$P\phi-P_{k,h}\phi\rightarrow 0 \text{ as } k,h\rightarrow 0.$$

Theorem 0.0.4. *The discretized scheme of Eqs.* **S1–S3** *is consistent.*

Proof. For a smooth function $\phi(t,x)$, we use Taylor's theorem to write

$$\frac{\phi^{n+1}-\phi^n}{\tau}=\frac{\partial\phi^n}{\partial t}+O(\tau)$$

and

$$\frac{1}{h^2}\delta^2\phi = \left(\frac{\partial^2\phi}{\partial x^2}+\frac{\partial^2\phi}{\partial y^2}\right)+O\left(h^2\right).$$

For PDE Eq. S1,

$$P\phi = \frac{\partial\phi}{\partial t} - D_{\mathrm{M}}\left(\frac{\partial^2\phi}{\partial x^2}+\frac{\partial^2\phi}{\partial y^2}\right) - \frac{\alpha r}{r+k}\phi,$$

with discretization

$$P_{k,h}\phi = \frac{\phi^{n+1}_{i,j}-\phi^{n}_{i,j}}{\tau} - \frac{D_{\mathrm{M}}}{h^2}\delta^2\phi^2_{i,j} - \frac{\alpha r^n_{i,j}}{r^n_{i,j}+k}\phi^{n+1}_{i,j}.$$

Then

$$P\phi - P_{k,h}\phi = \frac{\alpha r^n_{i,j}}{r^n_{i,j}+k}\left(\phi^{n+1}_{i,j}-\phi^{n}_{i,j}\right)+O\left(\tau+h^2\right).$$

Because $\alpha r^n_{i,j}/(r^n_{i,j}+k)$ is a constant for fixed r, and

$$\phi^{n+1}_{i,j}-\phi^{n}_{i,j} = \tau\frac{\partial\phi^n_{i,j}}{\partial t} + O\left(\tau^2\right) = O(\tau),$$

it follows that

$$P\phi - P_{k,h}\phi = O\left(\tau+h^2\right)\rightarrow 0 \text{ as } k,h\rightarrow 0,$$

and thus we verified consistency for our numerical scheme to solve Eq. **S1**. A similar argument applies to Eq. **S2**.

Let $f(\phi) = \alpha\phi/(\phi+k)$. For PDE Eq. **S3**,

$$P\phi = \frac{\partial\phi}{\partial t} - D_r\left(\frac{\partial^2\phi}{\partial x^2}+\frac{\partial^2\phi}{\partial y^2}\right) + f(\phi)(b_{\mathrm{M}}+b_{\mathrm{N}}),$$

with discretization

$$\begin{aligned}P_{k,h}\phi \;=\; &\frac{\phi^{n+1}_{i,j}-\phi^{n}_{i,j}}{\tau} - \frac{D_r}{h^2}\delta^2\phi^2_{i,j} + f\left(\phi^n_{i,j}\right)\\ &+ f'\left(\phi^n_{i,j}\right)\left(\phi^{n+1}_{i,j}-\phi^{n}_{i,j}\right)\left(b^n_{\mathrm{M},i,j}+b^n_{\mathrm{N},i,j}\right).\end{aligned}$$

Then

$$P\phi - P_{k,h}\phi = O\left(\tau+h^2\right) - f'\left(\phi^n_{i,j}\right)\left(\phi^{n+1}_{i,j}-\phi^{n}_{i,j}\right)\left(b^n_{\mathrm{M},i,j}+b^n_{\mathrm{N},i,j}\right),$$

and because $\phi^{n+1}_{i,j}-\phi^{n}_{i,j} = \tau\frac{\partial\phi^n_{i,j}}{\partial t} + O(\tau^2) = O(\tau)$, it follows that

$$P\phi - P_{k,h}\phi = O\left(\tau+h^2\right)\rightarrow 0 \text{ as } k,h\rightarrow 0.$$

The celebrated Lax–Richtmyer equivalence theorem (1) states that stability and consistency imply the following desirable property of the numerical solution:

Theorem 0.0.5. *As* τ *and* h *approach* 0, *the numerical solutions of Eqs.* **S1** *and* **S2** *converge to the actual solutions.*

The proof of consistency shows that the convergence order is one in time and two in space.

1. Berg HC (1993) *Random Walks in Biology* (Princeton Univ Press, Princeton).

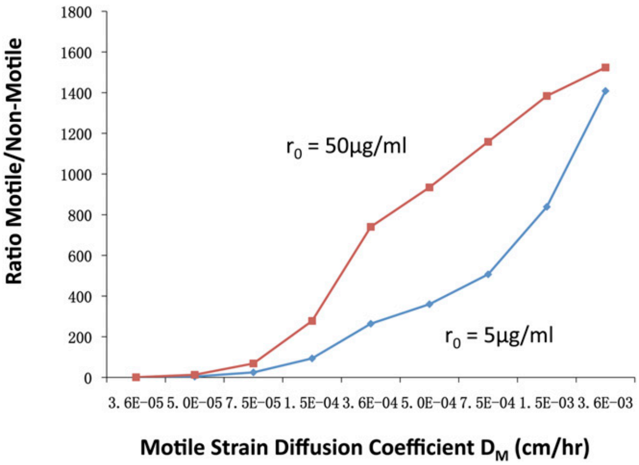

Fig. S1. Simulation of competition between motile and nonmotile cells in homogenous habitats with two different levels of resource and a fourfold larger matrix than in Fig. 1. Parameters: $\alpha = 0.90$ h^{-1}, $k = 5.0$ μg/mL, $\nu = 4.75 \times 10^{-7}$ μg, and $dt = 0.1$ h^{-1}. The computations used a grid size of 0.1 cm and the ratios were computed at the tick marks shown. The ratio of motile to nonmotile cells is shown for different motile strain diffusion coefficients D_{M} assuming $D_{\mathrm{R}} = 3.6 \times 10^{-3}$ and $D_{\mathrm{N}} = 3.6 \times 10^{-5}$ cm/h.

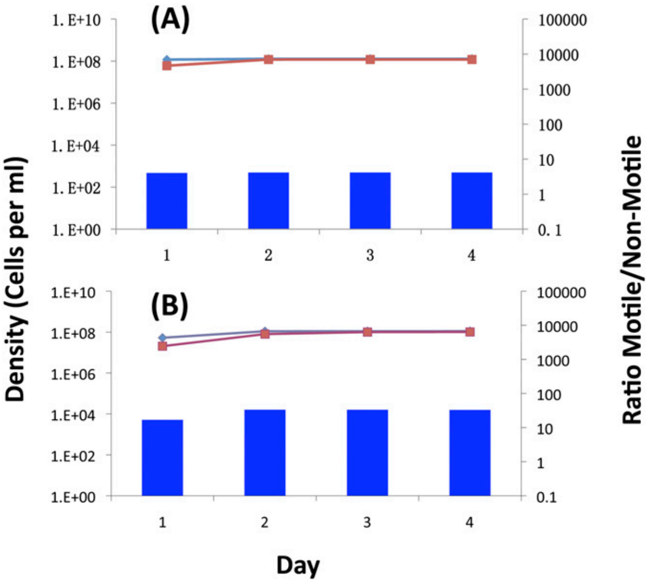

Fig. S2. Simulated changes in the density of motile (blue) and nonmotile strains (red) in single-clone culture and ratio of motile/nonmotile cells (*M*/*N* in right axis) in pairwise competition in 0.35% soft agar with $r_0 = 50$ μg/mL, $\alpha = 0.90$ h^{-1}, $k = 5.0$ μg/mL, $\nu = 4.75 \times 10^{-7}$ μg, and $dt = 0.1$ h^{-1}. (*A*) Culture initiated with 50 randomly distributed M and 50 N cells. (*B*) Culture initiated with mixtures of 50 M and 50 N cells randomly distributed as pairs.